# Study of structural, optical, and morphological characteristics of manganese titanate ($MnTiO_3$) obtained by combustion reaction using microwave energy

***R. C. V. Costa[1]*, G. N. Marques[2], T. P. Oliveira[2], M. M. Oliveira[2], J. H. G. Rangel[1]***
*[1]Instituto Federal de Ciência e Tecnologia do Maranhão, PPGQ, 65030-005, S. Luís, MA, Brazil*
*[2]Instituto Federal de Ciência e Tecnologia do Maranhão, PPGEM, S. Luís, MA, Brazil*

**Abstract**

$MnTiO_3$ is a semiconductor that has relevant dielectric and optical properties. For the synthesis of manganese titanate ($MnTiO_3$) powders, the combustion method via microwave and subsequent calcination at 500, 700, and 900 °C were used. The structural, morphological, and optical properties of the samples were investigated. X-ray diffraction analyzes were performed, where it was possible to index all peaks in the pyrophanite phase with a rhombohedral structure for the 900 °C sample. FTIR spectra corroborate the diffraction results, showing the presence of the vibrational modes characteristic of the $MnTiO_3$ bonds. SEM images revealed the formation of distorted nanobands with an average diameter of 320 nm. The optical spectrum obtained from the UV-vis absorption spectroscopy suggested a bandgap for $MnTiO_3$ of around 3.18 eV. The present work showed that combustion synthesis via microwave is efficient for the production of pure manganese titanate after calcination at 900 °C for 2 h.
**Keywords**: combustion synthesis, microwave, manganese titanate.

## INTRODUCTION

In recent years, research related to obtaining titanates has been widely studied due to the various properties attributed to this group of materials and consequently to the possibilities of application, such as the photoluminescence of $MgTiO_3$ systems doped with $Dy^{3+}$, the use of the $FeTiO_3$ composite for lithium storage, and the synthesis of $CoTiO_3$ doped with La for gas detection [1-3]. The band gap values of manganese titanate allow its application in solar cells, dielectric and piezoelectric ceramics, chemical sensors, magnetic materials, and photocatalysis [4]. $MnTiO_3$ is a compound of type $ABO_3$, in which A-site is occupied by a large atom, in the case of titanates generally a transition metal with radius and valence status according to the characteristics of the metal of B-site, titanium. This material can present both ilmenite and perovskite-type structures, and its crystallization under synthesis conditions depends on the type of synthesis, temperature, pressure, and composition [5, 6]. The synthesis of $MnTiO_3$-based powders generally occurs through the conventional method, which involves grinding the starting oxides and subsequent calcination. However, important properties can be affected by both the easy formation of secondary phases at temperatures below 700 °C and the use of high calcination temperatures (above 1200 °C) to avoid their formation [7].

The synthesis through the solution combustion (SC) method is a simple, efficient, and fast way in the production of powders with a high surface area, single-phase systems, and a high degree of purity [8]. The solution combustion method is based on thermodynamic studies that involve oxidation reactions between a fuel and metallic salts [9]. The quantities of the reagents used in the synthesis are obtained from the determination of the number of moles of urea necessary for the complete combustion of the system. Clark et al. [10] demonstrated that combustion synthesis can have an improved effect from the use of microwave radiation due to the mechanisms that act in the transfer of energy almost uniformly inside the sample. For this reason, combustion synthesis initiated in this way has considerable advantages over the conventional heating method using the muffle furnace, which was demonstrated in a study comparing the synthesis of lanthanum ferrite co-doped with strontium and copper ($La_{1-x}Sr_xFe_{1-y}Cu_yO_3$) by the conventional method and microwave energy [11]. In the same study, it was reported that the reduction in combustion time and the non-formation of secondary phases are associated with the direct interaction between microwave energy and the material.

The way the material is processed can have a significant effect on the properties of the product obtained. Some studies on the synthesis of manganese titanate revealed that the time spent with intermediate steps is generally high, in some cases exceeding 12 h [12]. Also, other factors that should be improved are the time and temperature of the calcination of the powders, which are generally around 900 °C and can take up to 6 h [12, 13]. So, this work used the microwave combustion method to decrease the time and temperature of the synthesis of manganese titanate and also as a way to evaluate the effects caused on the structural, morphological, and optical characteristics of the obtained powders.

**rayssacristina@acad.ifma.edu.br*
https://orcid.org/0000-0002-5864-4066

## EXPERIMENTAL

*Synthesis of $MnTiO_3$ powders*: the sample was prepared using stoichiometric amounts of 0.125 moles of titanium isopropoxide {$Ti[OCH(CH_3)_2]_4$, 98%, Aldrich} and 0.125 moles of manganese chloride ($MnCl_2.4H_2O$, RG, Neon), and as a fuel 0.125 moles of urea [$CO(NH_2)_2$, 99%, Synth]. The reagents were dissolved using 5 mL of distilled water in a beaker, with the aid of a stirring plate with a constant heating (70 °C) for 30 min. The solution remained in the microwave oven for 5 min, programmed with a maximum power of 900 W. After that period, the obtained material had a spongy appearance, which was then de-agglomerated in an agate mortar and calcined at 500, 700, and 900 °C for 2 h, with a heating rate of 10 °C.min$^{-1}$, under an ambient atmosphere in a muffle oven.

*Characterization of powders*: calcined samples were characterized by X-ray diffraction (XRD), using a diffractometer (Dmax 2500PC, Rigaku) with CuKα radiation (λ=1.5406 Å) in an angular range of 20° to 80° (2θ) with a scanning speed of 2 °/min. For identification of the structure, the obtained XRD patterns were compared and analyzed with JCPDS crystallographic files. Using the Scherrer equation, the crystallite size was calculated:

$$D = k.\lambda/(\beta.\cos\theta) \quad (A)$$

where D is the average crystallite size, k the shape factor that depends on the function used, λ the wavelength, θ the Bragg angle, and β the full width at half maximum (FWHM) of the peak (104) with the highest intensity. The data of the chemical bonds of the material were analyzed using a mixture composed of 1 wt% of each sample with 99 wt% of potassium bromide (KBr, 99%, Aldrich) using a Fourie-transform infrared (FTIR) spectrometer (Equinox 55, Bruker) with a resolution of 4 cm$^{-1}$. Micrographs of the sample were obtained using a scanning electron microscope with a field emission gun (SEM-FEG, Supra 35 VP, Carl Zeiss). The UV-vis spectroscopic measurements were performed in a spectrophotometer (Cary 5G, Varian) in diffuse reflectance mode. To calculate the energy of the optical gap ($E_{gap}$), the Wood and Tauc method was used, which relates the absorbance to the energy of the phonons by:

$$h\nu\alpha \propto (h\nu - E_{gap})^n \quad (B)$$

where α is the absorbance, h the Planck constant, ν the frequency, and n a constant that depends on the nature of the band transitions [14].

## RESULTS AND DISCUSSION

*XRD*: X-ray diffraction was performed to identify the crystalline phases formed and structural changes in the material. Fig. 1 shows the XRD patterns of the $MnTiO_3$ powders calcined at 500, 700, and 900 °C by the microwave-assisted combustion method. The XRD pattern of the 500 °C sample had a shallow halo, low crystallinity, and non-indexed peaks. For the sample treated at 700 °C, the widening at the base of the XRD peaks indicated a low crystallinity; however, it was possible to index the bixbyite-C, a cubic phase of manganese oxide (JCPDS 78-0390), common at this temperature [7], and the rutile phase, tetragonal titanium dioxide (JCPDS 89-0555), due to high stability of the rutile phase above 600 °C [15]. As for the sample treated at 900 °C, all XRD peaks were indexed as the pyrophanite phase with the spatial group R-3 and the rhombohedral structure of manganese titanate (JCPDS 89-3747), showing a good degree of long-term structural ordering. From thermodynamic calculations, it is possible to verify that at 900 °C, $Mn_2O_3$ and $TiO_2$ tend to react spontaneously, producing manganese titanate, in comparison to other manganese oxides (MnO, $Mn_3O_4$) due to their endothermic reactions [7]. No secondary phase was detected at this treatment temperature.

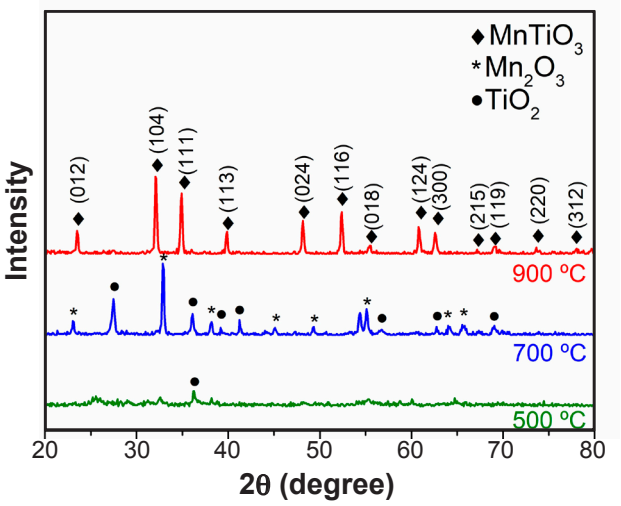


Figure 1: XRD patterns of samples synthesized for 2 h at different temperatures: a) 500 °C; b) 700 °C; and c) 900 ° C.

The average size of the crystallite, measured from the Scherrer formula, for the sample treated at 500 °C determined by the peak (220) was 18.8 nm. For the sample treated at 700 °C, it was determined from the peak (222) a value of 40.0 nm, and for the sample treated at 900 °C, the chosen peak was (104) and the size of the crystallite was 41.9 nm. So, it was noted the usual increase of the crystal size with the temperature [16]. Using the hydrothermal sol-gel method, it was possible to obtain $MnTiO_3$ at low temperatures, but with the need for mineralization in a reaction during 24 h [17]. Due to the non-identification of the XRD peaks and the presence of secondary phases, the other analyzes, such as FTIR and UV-vis spectroscopies, were not performed in the samples treated at 500 and 700 °C.

*FTIR*: Fig. 2 shows the FTIR spectrum of the powder synthesized by microwave at 900 °C for 2 h. The spectrum showed bands at 524 and 623 cm$^{-1}$ that were attributed to the vibrational modes of Mn-O-Ti and O-Ti-O, respectively, and

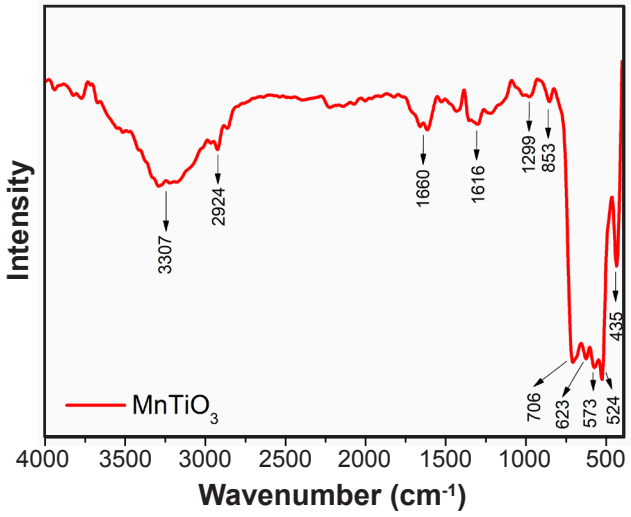


Figure 2: FTIR spectrum for the sample obtained at 900 °C/2 h.

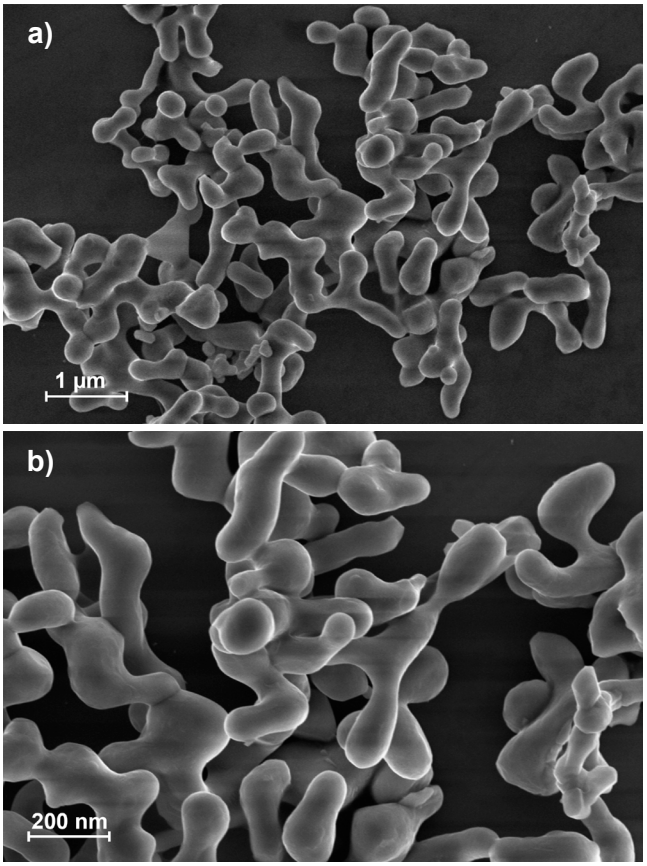


Figure 3: SEM micrographs of the powder obtained at 900 °C/2 h.

were very close to those obtained by Sharma et al. [18]. The bands located at 435, 573 and 706 $cm^{-1}$ were attributed to the vibrations of Ti-O [14, 19]. Vibrations characteristic of the residual organic compounds (C-H and C-O) were verified between 1600 and 850 $cm^{-1}$ [20]. Other vibrational modes present between 2800 and 3600 $cm^{-1}$ and at 1660 $cm^{-1}$ were characteristic of the O-H bonds of the adsorbed water on the sample surface [21].

*SEM-FEG*: Fig. 3 shows the SEM-FEG images of the $MnTiO_3$ sample calcined at 900 °C. The particles had an average diameter of 320 nm and the shape of distorted nanobands. The particle morphology was elongated with rounded edges and a smooth surface. A study [22] mapped a set of morphologies for $MnTiO_3$, starting from the truncated cylindrical shape; in addition, several others have been proposed. Due to the method used to obtain the sample, it was not possible to associate a theoretical morphology with that of the present study.

*UV-vis*: to determine the experimental energy value of the optical gap ($E_{gap}$), diffuse UV reflectance spectroscopy (DRS) was performed on the $MnTiO_3$ sample. To calculate $E_{gap}$, Eq. B was used [14, 23]. The photon absorption of the $MnTiO_3$ sample treated at 900 °C was located at a wavelength of around 396 nm in the UV region. The corresponding experimental value for indirect $E_{gap}$ was 3.18 eV (Fig. 4). This $E_{gap}$ value was consistent with those reported in the literature for pure $MnTiO_3$ [24]. The results also revealed a high reflectance in the visible region, which is characteristic of nanometric materials with particles of dimensions on the scale of the employed radiation. The electrons of the 3d layer of the $Mn^{2+}$ ions, since they are more external, interact with the crystal field or host crystal. Enhessari et al. [24] suggest that the electronic transitions attributed to $MnTiO_3$ are $^4T_1$ ($^4G$)→$^6A_1$, $^4T_2$ ($^4G$)→$^6A_1$, $^4E$ ($^4G$) and $^4A_1$ ($^4G$)→$^6A_1$, $^4T_2$ ($^4D$)→$^6A_1$, $^4E$ ($^4D$)→$^6A_1$.

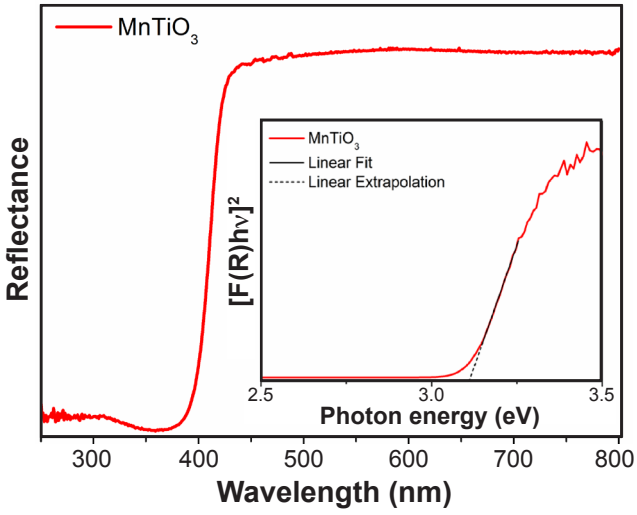


Figure 4: DRS spectrum of the heat-treated powder at 900 °C/2 h.

## CONCLUSIONS

The results showed that the combustion method via microwave was efficient in obtaining samples in a fast way. The formation of the single phase of the compound with the rhombohedral structure of $MnTiO_3$ was observed at the calcination temperature of 900 °C, as verified by XRD. The absorption bands found by FTIR spectroscopy showed the presence of Mn-O-Ti, O-Ti-O, and Ti-O vibrations in the 800-400 $cm^{-1}$ range. Through the images obtained by SEM-FEG, the average particle size around 320 nm was calculated. The samples showed an elongated morphology

with rounded edges. The UV-vis spectrum showed a 3.18 eV bandgap that was associated with an absorption in the ultraviolet region.

## ACKNOWLEDGMENTS

The authors acknowledge CAPES, IFMA, and LIEC-UFSCar laboratory.

## REFERENCES

[1] R.S. Yadav, Monika, E. Rai, L.P. Purohit, S.B. Rai, J. Lumin. **217** (2020) 116810.
[2] M. Siemons, U. Simon, Sens. Actuators B Chem. **120** (2006) 110.
[3] F. Zhang, Y. Chen, Q. Tian, Synth. Met. **260** (2020) 116302.
[4] H. Wang, Q. Gao, H.T. Li, M. Gao, B. Han, K.S. Xia, C.G. Zhou, ACS Appl. Nano Mater. **1** (2018) 2727.
[5] X. Wu, S. Qin, L. Dubrovinsky, Geosci. Front. **2** (2011) 107.
[6] J. Ko, N.E. Brown, A. Navrotsky, C.T. Prewitt, T. Gasparik, Phys. Chem. Miner. **16** (1989) 727.
[7] A.M. Abyzov, N.A. Khristyuk, F.M. Shakhov, Ceram. Int. **46** (2020) 1990.
[8] P. Heidari, S.M. Masoudpanah, J. Mater. Res. Technol. **9** (2020) 4469.
[9] S.M. Hashemi, D. Karami, N. Mahinpey, Fuel **269** (2020) 117432.
[10] D.E. Clark, I. Ahmad, R.C. Dalton, Mater. Sci. Eng. A **144** (1991) 91.
[11] R. Rosa, C. Ponzoni, P. Veronesi, I. Natali Sora, V. Felice, C. Leonelli, Ceram. Int. **41** (2015) 7803.
[12] S. Alkaykh, A. Mbarek, E.E. Ali-Shattle, Heliyon **6** (2020) e03663.
[13] M. Shaterian, M. Barati, K. Ozaee, M. Enhessari, J. Ind. Eng. Chem. **20** (2014) 3646.
[14] T. Acharya, R.N.P. Choudhary, Appl. Phys. A Mater. Sci. Process. **121** (2015) 707.
[15] V.Y. Zenou, S. Bakardjieva, Mater. Charact. **144** (2018) 287.
[16] R.K. Maurya, D. Singh, Mater. Lett. **246** (2019) 49.
[17] Z.-Q. Song, S.-B. Wang, W. Yang, M. Li, H. Wang, H. Yan, Mater. Sci. Eng. B **113** (2004) 121.
[18] Y.K. Sharma, M. Kharkwal, S. Uma, R. Nagarajan, Polyhedron **28** (2009) 579.
[19] L. Kernazhitsky, V. Shymanovska, T. Gavrilko, G. Puchkovska, V. Naumov, T. Khalyavka, V. Kshnyakin, V. Chernyak, J. Baran, Mater. Sci. Eng. B Solid-State Mater. Adv. Technol. **175** (2010) 48.
[20] O. Harizanov, T. Ivanova, A. Harizanova, Mater. Lett. **49** (2001) 165.
[21] B. Erdem, R.A. Hunsicker, G.W. Simmons, E. David Sudol, V.L. Dimonie, M.S. El-Aasser, Langmuir **17** (2001) 2664.
[22] R.A.P. Ribeiro, J. Andrés, E. Longo, S.R. Lazaro, Appl. Surf. Sci. **452** (2018) 463.
[23] M.M. Hue, N.Q. Dung, L.T.K. Phuong, N.N. Trung, N. Van Duc, L.H. Bac, D.D. Dung, J. Magn. Magn. Mater. **471** (2019) 164.
[24] M. Enhessari, A. Parviz, E. Karamali, K. Ozaee, J. Exp. Nanosci. **7** (2012) 327.
*(Rec. 16/03/2020, Rev. 13/06/2020, 16/07/2020, Ac. 20/07/2020)*